Journal of Radiotherapy in Practice

cambridge.org/jrp

Radiobiological assessment of nasopharyngeal cancer IMRT using various collimator angles and non-coplanar fields

G. Sharbo[1], B. Hashemi[1], M. Bakhshandeh[2] and A. Rakhsha[3]

[1]Department of Medical Physics, Faculty of Medical Sciences, Tarbiat Modares University, Tehran, Iran; [2]Department of Radiology Technology, Faculty of Allied Medical Sciences, Shahid Beheshti University of Medical Sciences, Tehran, Iran and [3]Department of Radiation Oncology, Faculty of Medical Sciences, Shahid Beheshti University of Medical Sciences, Tehran, Iran

Original Article

Cite this article: Sharbo G, Hashemi B, Bakhshandeh M, and Rakhsha A. (2021) Radiobiological assessment of nasopharyngeal cancer IMRT using various collimator angles and non-coplanar fields. *Journal of Radiotherapy in Practice* **20**: 168–175. doi: 10.1017/S1460396919000943

Received: 8 October 2019
Revised: 26 November 2019
Accepted: 29 November 2019
First published online: 12 February 2020

Key words:
angle of collimator; IMRT; nasopharyngeal carcinoma; non-coplanar field; treatment planning

Author for correspondence:
Bijan Hashemi, Department of Medical Physics, Faculty of Medical Sciences, Tarbiat Modares University, Al-Ahmad and Chamran Cross, Tehran 1411713116, Iran. Tel: +98-21-82883892. Fax: +98-21-88006544.
E-mail: bhashemi@modares.ac.ir

Abstract

Aim: The aim of this study was to evaluate clinical efficacy and radiobiological outcome of intensity-modulated radiation therapy (IMRT) modalities using various collimator angles and non-coplanar fields for nasopharyngeal cancer (NPC).

Materials and methods: A 70-Gy planning target volume dose was administered for 30 NPC patients referred for IMRT. Standard IMRT plans were constructed based on the target and organs at risk (OARs) volume; and dose constraints recommended by Radiation Therapy Oncology Group (RTOG). Using various collimator angles and non-coplanar fields, 11 different additional IMRT protocols were investigated. Homogeneity indexes (HIs) and conformation numbers (CNs) were calculated. Poisson and relative seriality models were utilised for estimating tumour control probability (TCP) and normal tissue complication probabilities (NTCPs), respectively.

Results: Various collimator angles and non-coplanar fields had no significant effect on HI, CN and TCP, while significant effects were noted for some OARs, with a maximum mean dose (D_{max}). No significant differences were observed among the calculated NTCPs of all the IMRT protocols. However, the protocol with 10° collimator angle (for five fields out of seven) and 8° couch angle had the lowest NTCP. Furthermore, the standard and some of non-coplanar IMRT protocols led to the reduction in OARs D_{max}.

Conclusions: Using appropriate standard/non-coplanar IMRT protocols for NPC treatment could potentially reduce the dose to the OARs and the probability of inducing secondary cancer in patients.

Introduction

Nowadays, intensity-modulated radiation therapy (IMRT) techniques are utilised as a powerful method for treating nasopharyngeal carcinoma (NPC). This therapeutic modality provides higher sparing of parotid glands at early stage of the disease as compared to the three-dimensional conformal radiation therapy (3D-CRT). Furthermore, IMRT has some advantages, including better tumour coverage, normal organ sparing and dose escalation in locally advanced diseases. Recent studies have used radiobiological modelling to compare different treatment plans.[1,2] According to such studies, IMRT provides better radiobiological outcome in terms of tumour control probability (TCP) and normal tissue complication probability (NTCP) for NPC. The most common complications associated with the radiation therapy of NPC are xerostomia and dysphagia due to the irradiation of parotid tissues, pharyngeal constrictors, oesophagus and larynx. The application of radiobiological models for evaluating and ranking the rival treatment plans will play a new role in radiation therapy planning. One of the disadvantages of IMRT are the increased number of radiation fields, more monitor units (MUs) and longer calculation time. Because of the greater number of radiation fields used in IMRT,[3] the amount of scattered and radiation leakage is higher than 3D-CRT. As a result, dose to organs at risk (OARs) is higher and the probability of secondary cancer is more compared to that in 3D-CRT.[4–12] In previous studies,[13,14] IMRT plans have been made for NPC patients, and homogeneity index (HI), conformity number (CN), TCP and NTCP are calculated based on the different radiobiological models. However, in such studies no optimal treatment plans have been proposed to reduce the D_{max} for OARs. In addition, optimising treatment planning of NPC is more complex because of involving more OARs. It was supposed that changing the collimator angles and using non-coplanar fields could play an important role in reducing the OARs. Therefore, our aim was to investigate the effects of using various collimator angles and also non-coplanar fields on the treatment planning indexes such as HI, CN and D_{max} of OARs. Standard and 11 different IMRT

CAMBRIDGE UNIVERSITY PRESS

Table 1. Details of the extra IMRT treatment planning protocols used for the NPC patients

Protocols	Fields and collimator angle (in °) combination	Couch angle (in degree)
1	7 Fields with collimator angle of 0	0
2	7 Fields with collimator angle of 5	0
3	7 Fields with collimator angle of 10	0
4	2 Fields with collimator angle of 5 + 5 fields with collimator angle of 0	4
5	2 Fields with collimator angle of 5 + 5 fields with collimator angle of 0	8
6	2 fields with collimator angle of 10 + 5 fields with collimator angle of 0	4
7	2 Fields with collimator angle of 10 + 5 fields with collimator angle of 0	8
8	5 Fields with collimator angle of 5 + 2 fields with collimator angle of 0	4
9	5 Fields with collimator angle of 5 + 2 fields with collimator angle of 0	8
10	5 Fields with collimator angle of 10 + 2 fields with collimator angle of 0	4
11	5 Fields with collimator angle of 10 + 2 fields with collimator angle of 0	8

Abbreviations: IMRT, intensity-modulated radiation therapy; NPC, nasopharyngeal cancer.

Table 2. The organ at-risk (OAR) constraints used for the dosimetric and radiobiologic assessment

	Constraints	
OAR	Maximum dose (Gy)	Dose volume
Brainstem	54	Less than 1% should receive up to 60 Gy if maximum dose cannot be achieved
Spinal cord	45	Less than 1% or 1 cc should receive up to 50 Gy if maximum dose cannot be achieved
Optic nerves/chiasm	54	Less than 1% should receive up to 60 Gy if maximum dose cannot be achieved
Parotid glands	28	Mean dose < 26 Gy or 50% volume to exceed 30 Gy if mean dose cannot be achieved

protocols were used for the treatment planning of patients with NPC. Based on the acquired dosimetric data from the protocols, radiobiological evaluation was also performed. In this regard, relative seriality (RS) model was used based on a series of parameters, including the TCP and NTCP. To select the best IMRT protocol for NPC treatment, the protocols were evaluated and compared with each other based on the calculated HI, CN, D_{max} for OARs, TCP and NTCP mean values.

Materials and Methods

Patient selection

This retrospective study was conducted on 30 patients with NPC, whose IMRT planning were made using the Eclipse treatment planning system (Eclipse TPS, version 13; Varian Company, USA) following Iranian National Research Ethics Board's approval. The patients whose tumours ranged from stage I to IV were selected for the study, consisting of 24 males and 6 females with age ranging from 18 to 67 years. All the IMRT plans were carried out using a Varian 6 MV photon beam modulated with 80 pairs of multi-leaf collimator (Varian 600c; Linear Accelerator, USA). All dose calculations were performed with the anisotropic analytical algorithm using a calculation grid of 2·5 mm. The accuracy of the Eclipse TPS has been previously evaluated for the small fields in IMRT.[15,16] A team comprising one radiation oncologist and one medical physicist generated the IMRT plans to avoid the variation in IMRT plan quality caused by the operator's experience and skill.

Treatment planning and modalities

For each patient, in addition to the standard IMRT plans, 11 additional treatment plans were generated using various collimator angles and also non-coplanar fields. Details of various protocols are presented in Table 1.

The plans were designed for a single treatment course of 33 sessions. Seven coplanar fields were used with an angle of 0, 50, 100, 150, 210, 260 and 310°. A dose of 70 Gy was used for nasopharyngeal primary and gross nodal disease as well as the required margins (planning target volume PTV_{70}). Additionally, a dose of 59·4 and 54 Gy were applied for the high-risk ($PTV_{59.4}$) and low-risk lymph nodes (PTV_{54}), respectively. For all the PTVs, a 5-mm margin was added to the clinical target volumes, except in the areas adjacent to the critical structures. The tolerance doses regarded for the normal tissues including brains team, spinal cord, optic nerves, optic chiasm and parotid glands were based on the recommendations proposed by Radiation Therapy Oncology Group (RTOG-0615) as presented in Table 2[17].

Treatment plan evaluation

The PTV dose coverage, OARs doses and also dose volume histograms were calculated using Eclipse TPS and used for treatment planning evaluation. In addition, extra treatment planning parameters were considered for evaluating the treatment plans, including conformation number (CN) describing the conformation of the dose to the target as defined by Equation (1)[18]:

https://doi.org/10.1017/S1460396919000943 Published online by Cambridge University Press

Table 3. The biological functions and additional constraints that are selected for the optimisation of NPC plans

Organ	D_{50}(Gy)	γ	s	α/β	Clinical endpoint
PTV	57·4	6·3	–	10	Local control
Brain stem	65·10	2·4	1	3	Necrosis/infarction
Spinal cord	68·60	1·9	4	3	Myelitis necrosis
Optic chiasm	65	2·3	1	3	Blindness
Optic nerve	65	2·3	1	3	Blindness
Parotid	46	1·8	1	3	Xerostomia

Abbreviations: NPC, nasopharyngeal cancer; PTV, planning target volume.

$$CN = \frac{TV_{RI}}{TV} \times \frac{TV_{RI}}{V_{RI}} \quad (1)$$

in which TV_{RI}, TV and V_{RI} represent the target volume covered by the reference isodose, target volume and volume of the reference isodose, respectively. The CN < 1 indicates that the target volume is not completely covered by the prescribed isodose volume, and CN > 1 indicates liberal coverage. However, a CN value close to 1 does not imply that the two volumes closely coincide spatially unless the PTV is completely contained within the prescription isodose volume. The HI indicates dose homogeneity in the target volumes, as recommended by the International Commission on Radiation Units and Measurements.[19] This index is defined as the ratio of the dose difference between the greatest dose delivered to 2% of the target volume ($D_{2\%}$) and the dose to 98% of the target volume ($D_{98\%}$) to the target median dose (D_{median}) as described in Equation (2):

$$HI = (D_{2\%} - D_{98\%})/D_{median} \quad (2)$$

Smaller HI values correspond to more homogenous target volume irradiation, with a value of 0 indicating absolute homogeneity of dose within the target.

Radiobiological treatment plan evaluation

The basic dose–response relation used for tumours and normal tissues in our study was based on the Poisson model described in previous reports[20–23] as presented in Equation (3):

$$P(D) = \exp\left(e^{e\gamma-(D_{2Gy}/D_{50})(e\gamma-\ln\ln 2)}\right) \quad (3)$$

where P(D) is the probability of tumour control or normal tissue complication when the tissue is irradiated uniformly with a dose D, D_{50} is the dose that induces a 50% response and γ is the maximum normalised dose–response gradient. As proposed by other researchers,[14] the values of the D_{50} and γ parameters are both organ and clinical endpoint dependent and are normally derived from clinical data as presented in Table 3.

These are in line with the recommendations from the quantitative analysis of normal tissue effects in the clinic reviews with regard to the clinical endpoints used and the dose–response relations for brainstem, spinal cord, optic nerves, optic chiasm and parotid glands.

As recommended by Monica et al.,[14] since the values of the radiobiological parameters are determined for a certain fractionation scheme, to compare the effectiveness of different dose distributions, they must be converted to the corresponding fractionation scheme. This is done in Equation (3) using the D_{2Gy} (that is also referred as EQD_{2Gy} in literature), which is a 2-Gy equivalent dose calculated using Equation (4) proposed by Komisopoulos et al.[20]:

$$D_{2Gy} = D \cdot \left(\frac{1+\frac{d}{\alpha/\beta}}{1+\frac{2}{\alpha/\beta}}\right) \quad (4)$$

where 2 Gy represents the reference dose level used for the determination of dose–response parameters, D is the physical dose, d is the dose per fraction and α/β is the organ-specific dose that accounts for the fractionation characteristics of the tissue and at which the linear and quadratic components of cell killing are equal. For estimating NTCP from nonuniform dose distribution, the RS model was used. Subsequently, the overall probability of injury, P_I, for a number of OARs was calculated using Equation (5)[24,25] as described below:

$$P_I = 1 - \prod_{j=1}^{N_{organs}} \left(1 - \left[1 - \prod_{i=1}^{M_j}\left(1 - P^j(D_i)^{S_j}\right)^{\Delta v_i}\right]^{1/S_j}\right) \quad (5)$$

where N_{organs} is the total number of vital OARs and $P^j(D_i)$ is the response probability of the organ j having the reference volume irradiated by a dose D_i as given by Equation (3). Furthermore, $\Delta v_i = \Delta V_i/V_{ref}$ is the fractional subvolume of the organ being irradiated compared to reference volume for which D_{50} and γ have been calculated, M_j is the total number of voxels or subvolumes in organ j and S_j is RS parameter characterising the internal organ structure of organ j. s = 1 indicates a serial structure tissue, whereas s = 0 indicates a tissue of parallel structure. NPC tumours are assumed to have a parallel structure since every clonogenic cell within the tumour volume must be destroyed. Consequently, TCP and the overall probability of benefit, P_B, were quantified using the Poisson model proposed in previous reports,[20,24,25] as described in Equation (6):

$$P_B = \prod_{j=1}^{N_{tumors}} \left(\prod_{i=1}^{M_j} P^j(D_i)^{\Delta v_i}\right) \quad (6)$$

where $N_{tumours}$ is the total number of tumours or targets involved in the clinical case.

Statistical analysis

Statistical analysis was performed with the Statistical Package for Social Science (SPSS), version 17.0, for Windows. All data are expressed as mean ± standard deviation. The analysis of variance with repeated measures was used. p Values less than 0·05 were considered as statistically significant.

https://doi.org/10.1017/S1460396919000943 Published online by Cambridge University Press

Table 4. The mean and standard deviation (SD) of the patients' OARs, TPTV and V_c volumes (in cm^3)

Patient no.	Vbs	Vsc	Voc	Vron	Vlon	Vrp	Vlp	V_{TPTV}	Vc
1	14·3	16·3	0·6	0·9	0·9	16·3	17·8	482·7	0·4
2	28·3	20·1	0·7	1·4	1·5	19·4	18·4	843·5	0·7
3	19·2	12·2	0·4	0·3	0·4	41·6	36·3	291·1	12·3
4	24·3	17·3	0·4	0·5	0·5	12·5	11·7	1052·6	5·7
5	17·2	15·4	0·4	0·1	0·2	30·5	29·3	873·5	22·0
6	24·2	14·0	0·0	0·2	0·2	15·2	12·1	1062·4	7·2
7	25·6	25·9	0·7	0·1	0·1	26·0	20·0	869·5	16·4
8	25·7	31·5	0·5	1·2	0·9	43·1	46·9	956·1	11·5
9	23·6	13·3	0·1	0·3	0·3	40·1	32·4	927·9	9·7
10	21·0	8·2	0·2	0·4	0·4	21·3	30·7	1013·1	6·1
11	22·5	11·7	0·4	0·3	0·2	17·8	15·8	1055·6	5·8
12	40·2	32·7	1·0	0·3	0·3	20·6	27·7	1232·3	5·1
13	18·7	28·2	0·8	0·3	0·3	12·4	6·5	725·0	0·1
14	16·5	19·5	0·8	1·0	1·0	4·2	3·7	182·2	0·0
15	29·8	50·0	0·9	1·0	1·6	25·7	19·1	758·1	1·2
16	20·0	38·1	0·5	0·3	0·1	14·4	15·5	1319·3	13·1
17	14·5	31·1	1·1	0·3	0·3	12·5	11·3	1306·3	0·0
18	23·4	55·9	1·5	0·4	0·2	14·6	15·9	973·5	8·8
19	29·4	48·5	0·5	0·3	0·2	20·8	22·2	1015·6	13·8
20	24·6	46·3	0·4	0·1	0·2	15·8	14·6	1000·5	8·7
21	22·6	13·2	0·3	0·3	0·5	13·4	15·1	1131·9	12·4
22	19·0	21·7	0·3	0·6	0·5	46·8	42·0	1087·2	17·7
23	16·4	9·4	0·7	0·4	0·3	23·8	17·7	786·9	3·0
24	25·7	40·2	0·5	0·0	0·1	31·9	35·9	1125·4	10·3
25	24·2	30·1	0·7	0·3	0·3	38·5	35·1	1243·3	12·2
26	25·3	39·7	0·7	0·7	0·7	11·4	9·6	1149·3	10·4
27	26·8	13·5	0·8	0·4	0·6	26·8	28·1	1053·5	6·7
28	20·0	16·3	1·1	0·5	0·3	16·3	20·6	1044·3	1·3
29	25·9	28·1	0·6	0·5	0·6	17·2	23·1	1041·0	2·3
30	23·8	18·8	1·3	0·3	0·3	38·5	30·7	2014·7	23·1
Mean ± SD	23·09 ± 5·27	25·57 ± 13·36	0·63 ± 0·34	0·45 ± 0·33	0·46 ± 0·37	22·98 ± 11·14	22·19 ± 10·67	987·27 ± 326·8	8·26 ± 6·44

Abbreviations: OAR, organ at risk; TPTV, total planning target volume.
V represents the volume of various OARs including brainstem (bs), spinal cord (sc), optic chiasm (oc), right optic nerve (ron), lift optic nerve (lon), right parotid (rp), left parotid (lp), TPTV and V_c.

Results

Patient characteristics, PTV and OAR volume

For the 30 patients with NPC selected in our study, the mean volumes for total PTV (TPTV) and OARs are presented in Table 4. These patients had a feature of having a common volume V_c between their TPTV and parotids glands.

Analyses of HI and CN

The patients' HI and CN of the PTV-70 and PTV-59.4 calculated for all the investigated protocols are presented in Table 5. As could be noted from the results of statistical analysis carried over the mean values of HI and CN, no significant differences regarding these parameters are observed among various protocols.

Dose analysis of OAR

Table 6 describes the patients' mean D_{max} received by the brainstem, spinal cord, optic nerves and parotid glands using different IMRT protocols. In general, the maximum doses of OAR_s were achieved based on the protocol of dose criteria recommended in RTOG-0615.[17] However, comparing various protocols with each other indicated different doses for some organs, including the optic chiasm, spinal cord, right optic nerve and right parotid gland. For the optic chiasm, protocol 1 (seven fields with collimator angle of 0 and couch

https://doi.org/10.1017/S1460396919000943 Published online by Cambridge University Press

Table 5. Comparison of the patients' HI and CN (mean ± SD) in terms of various IMRT protocols with relevant *p* values

Protocols	HI_{70}	CN_{70}	$HI_{59·4}$	$CN_{59·4}$
1	0·124 ± 0·007	0·748 ± 0·021	0·294 ± 0·008	0·286 ± 0·112
2	0·123 ± 0·007	0·751 ± 0·022	0·291 ± 0·007	0·285 ± 0·113
3	0·120 ± 0·007	0·755 ± 0·022	0·287 ± 0·006	0·286 ± 0·113
4	0·123 ± 0·007	0·758 ± 0·021	0·290 ± 0·007	0·284 ± 0·111
5	0·122 ± 0·007	0·756 ± 0·020	0·287 ± 0·006	0·287 ± 0·113
6	0·122 ± 0·007	0·755 ± 0·020	0·289 ± 0·007	0·287 ± 0·114
7	0·122 ± 0·007	0·757 ± 0·020	0·288 ± 0·006	0·287 ± 0·114
8	0·123 ± 0·007	0·755 ± 0·020	0·291 ± 0·007	0·285 ± 0·113
9	0·124 ± 0·007	0·757 ± 0·020	0·290 ± 0·007	0·287 ± 0·114
10	0·123 ± 0·007	0·754 ± 0·022	0·286 ± 0·008	0·286 ± 0·114
11	0·122 ± 0·007	0·755 ± 0·022	0·290 ± 0·007	0·286 ± 0·114
p Value	0·556	0·191	0·401	0·580

Abbreviations: HI, homogeneity index; CN, conformation number.

Table 6. The mean ± SD values of D_{max} (in Gy) for various OARs resulted from various protocols with relevant *p*-values

Protocols	D_{max}(bs)	D_{max}(*sc*)	D_{max}(oc)	D_{max}(ron)	D_{max}(lon)	D_{max}(rp)	D_{max}(*lp*)
1	50·117 ± 0·499	43·563 ± 0·415	29·167 ± 17·64	30·180 ± 3·239	30·288 ± 18·474	30·640 ± 1·045	34·864 ± 1·360
2	50·257 ± 0·504	43·451 ± 0·347	30·696 ± 16·46	30·748 ± 3·079	30·943 ± 16·658	30·562 ± 1·080	34·491 ± 1·398
3	50·090 ± 0·490	42·719 ± 0·346	32·208 ± 15·69	31·956 ± 3·056	31·217 ± 16·220	30·454 ± 1·053	34·441 ± 1·436
4	50·133 ± 0·453	42·894 ± 0·366	29·361 ± 17·60	29·694 ± 3·279	29·761 ± 16·165	30·532 ± 1·094	34·688 ± 1·360
5	49·946 ± 0·446	42·833 ± 0·360	29·553 ± 17·08	30·210 ± 3·269	30·222 ± 18·094	30·617 ± 1·081	34·649 ± 1·342
6	50·041 ± 0·438	43·022 ± 0·388	29·884 ± 17·20	29·991 ± 3·239	30·044 ± 17·944	30·564 ± 1·087	34·685 ± 1·341
7	50·038 ± 0·408	42·822 ± 0·361	29·897 ± 17·20	30·067 ± 3·257	30·104 ± 17·998	30·556 ± 1·096	34·683 ± 1·349
8	50·153 ± 0·463	42·562 ± 0·321	29·967 ± 17·30	30·429 ± 3·261	30·140 ± 17·868	30·429 ± 1·053	34·572 ± 1·348
9	50·121 ± 0·448	42·469 ± 0·324	30·033 ± 17·25	30·796 ± 3·197	30·452 ± 17·728	30·356 ± 1·050	34·458 ± 1·335
10	50·005 ± 0·476	42·180 ± 0·470	31·147 ± 16·48	31·093 ± 3·162	30·695 ± 17·276	30·248 ± 1·087	34·490 ± 1·336
11	50·230 ± 0·464	42·417 ± 0·367	30·970 ± 16·44	31·341 ± 3·156	30·923 ± 17·379	30·228 ± 1·086	34·586 ± 1·360
p-value	0·938	0·001	0·01	0·001	0·362	0·042	0·203

Abbreviation: OAR, organ at risk.

angle of 0) had the least mean D_{max} of 29·16 Gy ($p = 0·01$). For the right optic nerve, protocol 4 (2 fields with collimator angle of 5 + 5 fields with collimator angle of 0, couch angle of 4) had the least mean D_{max} 29·69 Gy ($p = 0·001$). For the spinal cord, protocol 10 (five fields with collimator angle of 10 + 2 fields with collimator angle of 0 and couch angle of 4) had the least mean D_{max} of 42·18 Gy ($p = 0·001$). For the right parotid gland, protocol 11 (5 fields with collimator angle of 10 + 2 fields with collimator angle of 0 and couch angle of 8) had the least mean D_{max} of 30·22 Gy ($p = 0·042$). But for other organs including the brainstem, left optic nerve and left parotid gland, no statistical differences were observed among the mean of D_{max}resulted from different protocols.

Analyses of TCP and NTCP

The calculated TCPs of NPC for all the protocols are presented in Table 7. The TCP was estimated using the Biosuite software based on Poisson model.[26] Table 7 shows no statistically significant differences between the protocols ($p = 0·658$). However, a better coverage of PTV and higher target dose was achieved with the protocol 5 (2 fields with a collimator angle of 5 + 5 fields with a collimator angle of 0 and a couch angle of 8°).

The calculated NTCPs derived from all of the OARs are presented in Table 8. The NTCP was estimated using the Biosuite software based on RS model.[26,27] Table 8 shows no statistically significant difference between the protocols ($p = 0·295$). However, the least NTCP value was achieved with the protocol 11 (5 fields with a collimator angle of 10 plus 2 fields with a collimator angle of 0 and a couch angle of 8°).

Discussion

It is well known that treatment planning for patients with NPC using IMRT is the most complex technique due to the small volume being treated and the presence of many important OARs that

https://doi.org/10.1017/S1460396919000943 Published online by Cambridge University Press

Table 7. TCP ± SD values for various IMRT protocols (70 Gy) based on Poisson model for all the NPC patients

Protocols	TCP %
1	93·87 ± 1·03
2	93·76 ± 1·02
3	94·36 ± 0·97
4	94·23 ± 0·90
5	94·71 ± 0·86
6	94·14 ± 1·16
7	93·75 ± 1·25
8	94·56 ± 0·88
9	94·46 ± 0·93
10	93·83 ± 0·98
11	93·54 ± 1·05
p-value	0·658

Abbreviations: TCP, tumour control probability; SD, standard deviation; IMRT, intensity-modulated radiation therapy; NPC, nasopharyngeal cancer.

Table 8. NTCP ± SD values for various IMRT protocols based on relative seriality model for all the NPC patients

Protocols	NTCP %
1	33·428 ± 3·105
2	32·946 ± 3·215
3	33·236 ± 3·130
4	33·391 ± 3·208
5	33·302 ± 3·231
6	33·825 ± 3·181
7	33·865 ± 3·210
8	33·413 ± 3·153
9	33·075 ± 3·157
10	32·903 ± 3·206
11	32·635 ± 3·204
p-value	0·295

Abbreviations: NTCP, normal tissue control probability; SD, standard deviation; IMRT, intensity-modulated radiation therapy; NPC, nasopharyngeal cancer.

may have a common volume with the PTV. Commonly in radiotherapy centres, the treatment plan for the NPC patient is made with a random selection of the collimator and couch angles, because systemic selection of these angles requires a long time to calculate during the treatment, which is costly and not practical. Previous studies have shown that treatment plans for the patients using IMRT are causing a high risk of secondary cancer later.[4–12] For this reason, in the present study, the effect of changing the collimator and couch angles on the treatment plans was studied. The main objective of the study was to reach an ideal protocol that provides the best coverage for the tumour and low dose for the OARs. From dosimetric point of view, all the studied protocols had almost the same coverage of the PTV without any statistical differences. The most important effect of changing the collimator

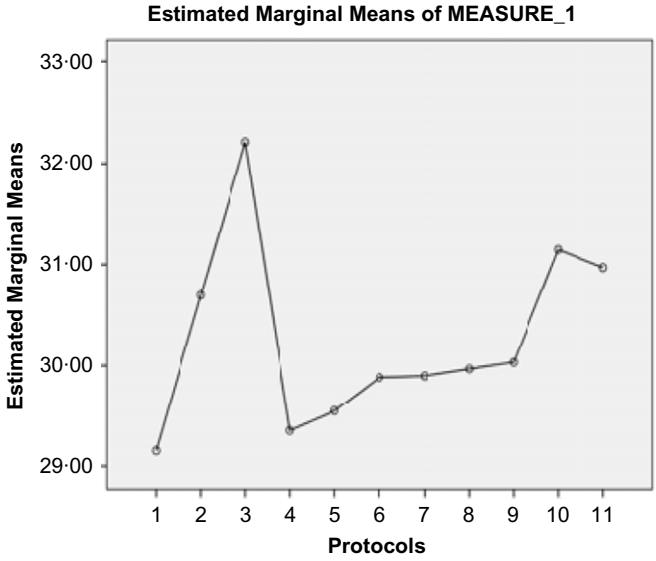

Figure 1. Variation in the mean D_{max} for the optic chiasm from all protocols.

and couch angles was observed in the D_{max} for some of the OARs. The comparison between the protocols showed statistically significant variation in the mean of D_{max} for the optic chiasm, spinal cord, right optic nerve and right parotid gland.

Figure 1 shows the mean of D_{max} for the optic chiasm for all the protocols. It is noted that protocol 1 (seven fields with collimator angle of 0 and couch angle of 0) has the lowest D_{max} of 29·16 ($p = 0·01$), with a regression equation of:

$$11.361 + 0.029\,(V_{TPTV}) - 1.323\,(V_{oc}) \quad (7)$$

in which V_{TPTP} and V_{oc} represent the mean volumes of TPTV and common volume between the TPTV and optic chiasm. Equation (7) implies that when the other independent variables in the model are kept constant, 1 unit increase in the V_{TPTP} variable leads to 0·029 unit increase, while 1 unit increase in the V_c leads to 1·323 decrease in the response. Therefore, this specific IMRT protocol could be considered for maintaining the maximum dose of the optic chiasm low in treating NPC patients. However, we must pay attention that while the total PTV has a small positive effect, the common volume of the target and optic chiasm has a large negative effect on the relevant regression response of this IMRT technique.

Figure 2 shows the mean of D_{max} for the spinal cord for all the protocols. It is noted that protocol 10 (5 fields with collimator angle of 10 + 2 fields with collimator angle of 0 and couch angle of 4) has the lowest D_{max} of 42·18 ($p = 0·001$), with a regression equation of:

$$40.211 + 0.077\,(V_{sc}) \quad (8)$$

in which V_{sc} represents the mean volume of the spinal cord. Equation (8) implies that 1 unit increase in the V_{sc} variable leads to 0·077 unit increase in the response. Therefore, this specific IMRT protocol could be considered to maintain the maximum dose of the spinal cord low in treating the NPC patients. However, we must pay attention that the mean volume of the spinal cord has a small negative effect on the relevant regression response of this IMRT technique.

https://doi.org/10.1017/S1460396919000943 Published online by Cambridge University Press

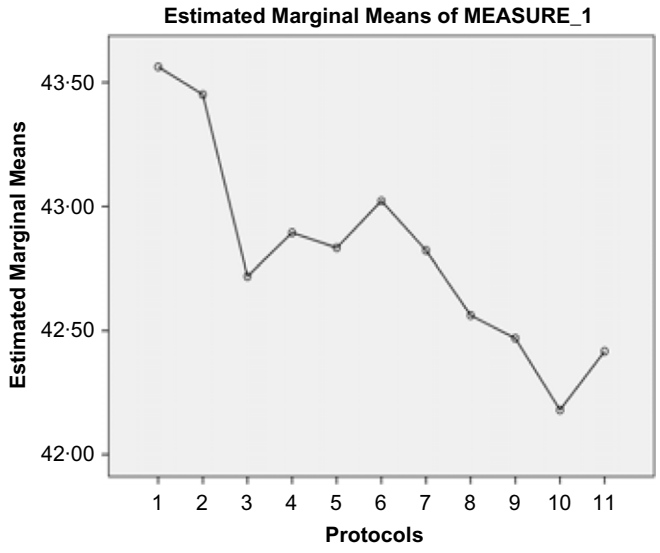

Figure 2. Variation in the mean of D_{max} for the spinal cord from all protocols.

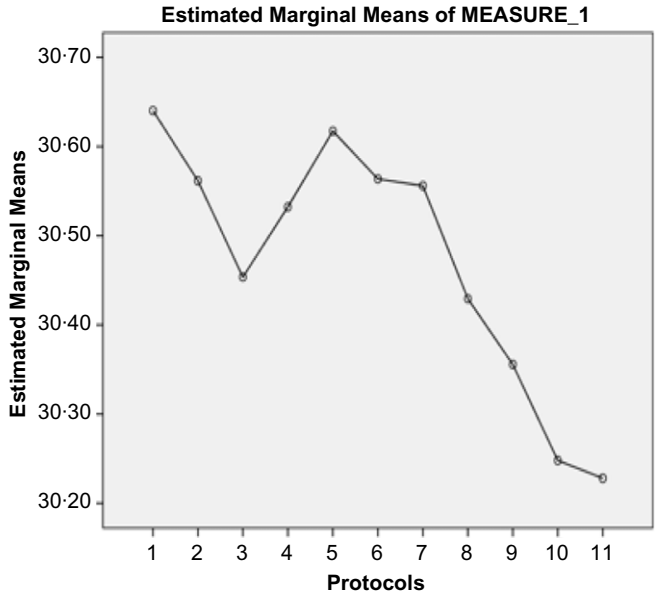

Figure 4. Variation in the mean of D_{max} for the right parotid gland from all protocols.

Figure 3 shows the mean of D_{max} for the right optic nerve for all protocols. It is noted that protocol 4 (2 fields with collimator angle of 5 + 5 fields with collimator angle of 0 and couch angle of 4) has the lowest D_{max} of 29·69 (p = 0·001), with a regression equation of:

$$7.936 - 14.916\ (V_{oc}) + 25.639\ (V_{lon}) - 0.708(V_{lp}) + 0.035(V_{TPTV}) \quad (9)$$

in which V_{oc}, V_{lon}, V_{lp} and V_{TPTV} represent the mean volumes of optic chiasm, left optic nerve, left parotid gland and total PTV, respectively. Equation (9) implies that when the other independent variables in the model are kept constant, 1 unit increase in the V_{TPTV} and V_{lon} variables lead to 0·035 and 25·639 unit increase, respectively; while 1 unit increase in the V_{oc} and V_{lp} lead to 14·916 and 0·708 decrease, respectively, in the response.

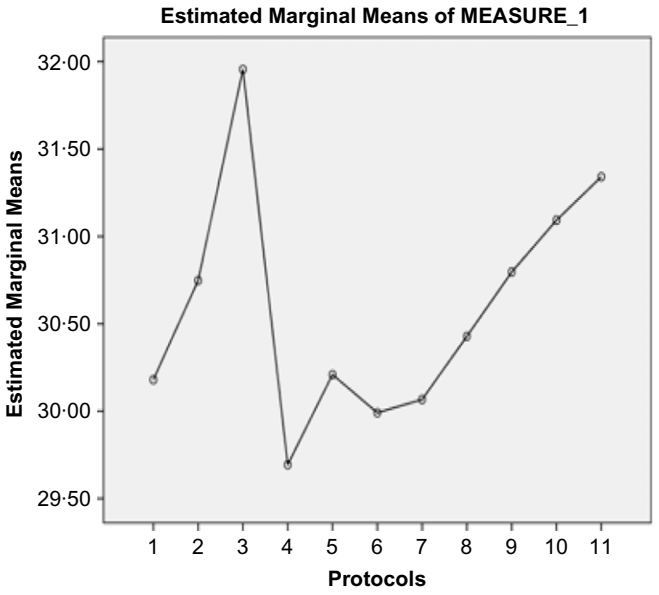

Figure 3. Variation in the mean of D_{max} for the right optic nerve from all protocols.

Therefore, this specific IMRT protocol could be considered for keeping the maximum dose of the right optic nerve low in treating the NPC patients. However, attention must be given when the optic chiasm and left parotid mean volumes have a large and small negative effect, and the left optic nerve volume and the total PTV have a large and small positive effect on the relevant regression response of this IMRT technique.

Figure 4 shows the mean of D_{max} for the right parotid gland for all protocols. It is noted that protocol 11 (5 fields with collimator angle of 10 + 2 fields with collimator angle of 0 and couch angle of 8) has the lowest D_{max} value of 30·22 ($p = 0·042$), with a regression equation of:

$$31.279 + 0.667\ (V_{oc}) - 2.96\ (V_{lp}) \quad (10)$$

Equation (10) implies that when the other independent variables in the model are kept constant, 1 unit increase in the V_{oc} variable leads to 0·667 unit increase, while 1 unit increase in the V_{lp} leads to 2·96 decrease in the response. Therefore, this specific IMRT protocol could be considered for keeping the maximum dose of the right parotid gland low in treating the NPC patients. However, we must pay attention that while the optic chiasm volume has a small positive effect, the left parotid volume has a large negative effect on the relevant regression response of this IMRT technique.

Our study included 12 IMRT protocols of interest including a standard common 7-field protocol (with no collimator and couch angle) and 11 additional 7-field protocols with various combinations of collimator (0, 5, 10) as well as couch[4,8] angles on a limited number of 30 patients. Similar studies on more number of patients at other radiotherapy centres could help to ascertain our results.

However, our study confirmed that although none of the 12 various IMRT protocols of interest has any significant effect on the highest dose delivered to the target, four specific protocols could be considered appropriate for keeping the maximum dose of some OARS including the optic chiasm, spinal cord, right optic nerve and right parotid gland at the lowest level with relevant

https://doi.org/10.1017/S1460396919000943 Published online by Cambridge University Press

regression equations including affecting parameters as described in Equations (7–10).

Conclusions

Based on the results and discussion presented above, it could be concluded that from all of the 12 various IMRT protocols investigated for the treatment planning of NPC patients, 4 protocols (1, 4, 10 and 11) could help us to reduce the D_{max} for some of the OARs. Although the statistical analysis showed no significant difference between the NTCPs of all the protocols ($p = 0{\cdot}938$), protocol 11 (5 fields with collimator angle of $10 + 2$ fields with collimator angle of 0 and couch angle of 8) indicated the lowest NTCP value compared to all other investigated protocols.

Considering the overall points discussed above and the conclusions made from our extensive studies, the various IMRT protocols for NPC treatment procedure could potentially reduce the secondary effects that might later appear after the treatment in clinical practice.

Acknowledgements. This research was carried out by the first author under the supervision of the second author and with the help and advice of the third and fourth authors for the project conducted at Tarbiat Modares University. The patients' imaging and their radiotherapy planning procedures were carried out at the radiotherapy and oncology department of Shohaday-e-Tajrish hospital, Tehran, Iran. Therefore, the authors express their sincere appreciation to the above institutes for their financial help and technical assistance.

Financial support. This research received no specific grant from any funding agency, commercial or not-for-profit sectors.

References

1. Narayanasamy G, Pyakuryal AP, Pandit S et al. Radiobiological evaluation of intensity modulated radiation therapy treatments of patients with head and neck cancer: a dual-institutional study. J Med Phys 2015; 40 (3): 165–169.
2. Wu PM, Chua DT, Sham JS et al. Tumor control probability of nasopharyngeal carcinoma: a comparison of different mathematical models. Int J Radiat Oncol Biol Phys 1997; 37 (4): 913–320.
3. NCI. The national cancer institute guidelines for the use of IMRT in clinical trials. http://rpc.mdanderson.org/RPC/services/Anthropomorphic_%20Phantoms/IMRT_NCI_Guidelines_v4.0.pdf. Accessed on 26th November 2019.
4. Tao Y, Lefkopoulos D, Ibrahima D et al. Comparison of dose contribution to normal pelvic tissues among conventional, conformal and intensity-modulated radiotherapy techniques in prostate cancer. Acta Oncol 2008; 47 (3): 442–450.
5. Fiandra C, Filippi AR, Catuzzo P et al. Different IMRT solutions vs. 3D-conformal radiotherapy in early stage Hodgkin's Lymphoma: dosimetric comparison and clinical considerations. Radiation Oncol 2012; 7 (1): 186.
6. Hall EJ, Wuu CS. Radiation-induced second cancers: the impact of 3D-CRT and IMRT. Int J Radiat Oncol Biol Phys 2003; 56 (1): 83–88.
7. Brenner DJ, Curtis RE, Hall EJ, Ron E. Second malignancies in prostate carcinoma patients after radiotherapy compared with surgery. Cancer 2000; 88 (2): 398–406.
8. Sigurdson AJ, Jones IM. Second cancers after radiotherapy: any evidence for radiation-induced genomic instability? Oncogene 2003; 22 (45): 7018–7027.
9. Dores GM, Metayer C, Curtis RE et al. Second malignant neoplasms among long-term survivors of Hodgkin's disease: a population-based evaluation over 25 years. Int J Clin 2002; 20 (16): 3484–3494.
10. Travis LB, Andersson M, Gospodarowicz M et al. Treatment-associated leukemia following testicular cancer. J Natl Cancer Inst 2000; 92 (14): 1165–1171.
11. Travis LB, Gospodarowicz M, Curtis RE et al. Lung cancer following chemotherapy and radiotherapy for Hodgkin's disease. J Natl Cancer Inst 2002; 94 (3): 182–192.
12. Richie JP, Travis LB, Fossa SD et al. Second cancers among 40,576 testicular cancer patients: focus on long-term survivors. Urol Oncol 2006; 24 (2): 171–171.
13. Boughalia A, Marcie S, Fellah M, Chami S, Mekki F. Assessment and quantification of patient set-up errors in nasopharyngeal cancer patients and their biological and dosimetric impact in terms of generalized equivalent uniform dose (gEUD), tumour control probability (TCP) and normal tissue complication probability (NTCP). Br J Radiol 2015; 88 (1050): 20140839.
14. Monica W. K. Kan, Lucullus H. T. Leung, Peter K. N. Yu. The use of biologically related model (Eclipse) for the intensity-modulated radiation therapy planning of nasopharyngeal carcinomas. PLoS ONE 2014; 9 (11): e112229.
15. Mesbahi A, Dadgar H. Dose calculations accuracy of TiGRT treatment planning system for small IMRT beamlets in heterogeneous lung phantom. Int J Radiat Res 2015; 13 (4): 345–354.
16. Mesbahi A, Zergoug I. Dose calculations for lung inhomogeneity in high-energy photon beams and small beamlets: a comparison between XiO and TiGRT treatment planning systems and MCNPX Monte Carlo code. Iran J Med Phys2015; 12 (3): 167–177.
17. Radiation Therapy Oncology Group. RTOG 0615: a phase II study of concurrent chemoradiotherapy using three – dimensional conformal radiotherapy (3D-CRT) or Intensity – Modulated Radiation Therapy (IMRT) + Bevacizumab (BV) for locally or regionally advanced Nasopharygeal Cancer. https://www.nrgoncology.org/Clinical-Trials/Protocol/rtog-0615?filter=rtog-0615%22. Accessed on 1st February 2020.
18. Van't Riet A, Mak AC, Moerland MA, Elders LH, Van Der Zee W. A conformation number to quantify the degree of conformality in brachytherapy and external beam irradiation: application to the prostate. Int J Radiat Oncol Biol Phys 1997; 37 (3): 731–736.
19. Landberg T, Chavaudra J, Dobbs J et al. ICRU report 62: prescribing, recording and reporting photon beam therapy (supplement to ICRU report 50). Bethesda MD: ICRU, 1999.
20. Komisopoulos G, Mavroidis P, Rodriguez S et al.. Radiobiologic comparison of helical tomotherapy, intensity modulated radiotherapy, and conformal radiotherapy in treating lung cancer accounting for secondary malignancy risks. Med Dosim 2014; 39 (4): 337–347.
21. Ågren A, Brahme A, Turesson I. Optimization of uncomplicated control for head and neck tumors. Int J Radiat Oncol Biol Phys 1990; 19 (4): 1077–1085.
22. Källman P, Ågren A, Brahme A. Tumour and normal tissue responses to fractionated non-uniform dose delivery. Int J Radiat Biol 1992; 62 (2): 249–262.
23. Lind BK, Mavroidis P, Hyödynmaa S, Kappas C. Optimization of the dose level for a given treatment plan to maximize the complication-free tumor cure. Acta Oncol 1999; 38 (6): 787–798.
24. Kallman P, Lind BK, Brahme A. An algorithm for maximizing the probability of complication-free tumour control in radiation therapy. Phys Med Biol 1992; 37 (4): 871–890.
25. Mavroidis P, Lind BK, Brahme A. Biologically effective uniform dose (D) for specification, report and comparison of dose response relations and treatment plans. Phys Med Biol 2001; 46 (10): 2607–2630.
26. Uzan J, Nahum AE. Radiobiologically guided optimisation of the prescription dose and fractionation scheme in radiotherapy using BioSuite. Br J Radiol. 2012; 85 (1017): 1279–1286.
27. Mesbahi A, Oladghaffari M. An overview on the clinical application of radiobiological modeling in radiation therapy of cancer. Int J Radiol Radiat Therapy 2017; 2 (1): 9–14.

https://doi.org/10.1017/S1460396919000943 Published online by Cambridge University Press